Calculation of vertical force between finite, cylindrical magnets and superconductors

E. Várguez-Villanueva[a], V. Rodríguez-Zermeño[b], and V. Sosa[a,*]
[a] *Universidad Autónoma de Yucatán, Facultad de Ingeniería, Av. Industrias no Contaminantes por Anillo Periférico Norte S/N, Apartado Postal 150 CORDEMEX, Mérida, México.*
[b] *Universidad Autónoma de S.L.P., Facultad de Ciencias, Av. Salvador Nava S/N, San Luis Potosí, México.*

Recibido el 17 de diciembre de 2007; aceptado el 22 de abril de 2008

The maximum force between a permanent magnet and a superconductor in the Meissner state has been calculated. The calculation was performed assuming the superconductor to be a perfect diamagnet and neglecting the London penetration depth. The resulting force takes into account the geometric dimensions of both the magnet and the superconductor. This constitutes an important improvement for the description of the maximum force attainable in these systems. The method can be applied in cases with azimuthal symmetry.

Keywords: Levitation; YBCO; Meissner effect.

Se calculó la máxima fuerza entre un imán permanente y un superconductor en el estado Meissner. El cálculo se realizó suponiendo que el superconductor es un diamagneto perfecto y despreciando la longitud de penetración de London. La fuerza resultante toma en cuenta las dimensiones geométricas tanto del imán como del superconductor. Esto constituye una mejora importante para la descripción de la máxima fuerza obtenible en estos sistemas. El método puede ser aplicado en casos con simetría azimutal.

Descriptores: Levitación; YBCO; efecto Meissner.

PACS: 85.25.Ly; 74.25.Ha

1. Introduction

Levitation of a permanent magnet over a high-Tc superconducting sample is a fascinating demonstration of the magnetic properties of these materials. This characteristic can be applied mainly to superconducting bearings [1]. Two main regimes of the superconducting levitation are typically defined. In the first case, the magnetic induction is expelled from the superconductor because of the Meissner effect. Under these circumstances the repulsive force reaches its maximum possible value, but the levitation is unstable. The second situation corresponds to the mixed state, where a partial penetration of magnetic lines occurs. The repulsive force diminishes because of this penetration, but due to the pinning of the magnetic lines in the inhomogeneities of the superconducting material, a desired mechanical stability is achieved.

The force in a magnet-superconductor system depends mainly on the quality of the sample, particularly on its capability to screen the external field. This is determined by the critical density current (Jc) of the material: the higher the Jc, the greater the repulsion. However, the physical characteristics of the magnet are important also. The critical current density can be increased by lowering the temperature of the sample. For example, Moon [2] reported a seven-fold increase of the force on a melt-textured superconductor when it was cooled from 77 to 10 K. Also, implantation of high-energy particles in the superconductor improves the effectiveness of the pinning centers and increases the Jc value. The high-Tc superconductor most commonly found in the literature in experimental studies of magnetic forces is $YBa_2Cu_3O_x$ (YBCO), but also there are some reports on $SmBa_2Cu_3O_x$ (SmBCO).

Some calculations of the levitation force between a permanent magnet and a superconductor in the mixed state have been performed [3-5]. In these papers, the authors used numerical methods. The calculations are parameterized by the Jc value.

To answer the question of how much the levitation force can be increased, one must go to the Meissner limit where a complete exclusion of magnetic field is assumed. This is equivalent to neglecting the London penetration depth, or taking an infinite Jc. Furthermore, it is desirable to obtain analytical expressions of this maximum force.

The simplest model of the vertical force considers the magnet to be a point dipole, and the superconductor to be a perfectly screened semi-infinite sample [6]. Models which considered finite one-dimensional superconductors were reported later [7,8]. There exist only a few studies about forces on finite superconductors in the Meissner state [9, 10].

Another model [11] studied the interaction between a point dipole (magnet) and a finite-size superconducting sample by integrating the dipole-dipole interactions all over the sample. Only the horizontal and vertical orientation of the magnetic moment of the magnet were considered in that study.

In the last few years, the dipole-dipole interaction model has been used in several papers. For example, it was useful to analyze the vertical force at any orientation of the magnet [12, 13]. Also, it was used to calculate the levitation force [14] and the lateral force [15] between a small magnet

and a cylindrical superconducting sample, between a small magnet and a superconducting ring [16], and between a small magnet and a superconducting square [17]. Vertical vibrations in these systems have also been studied following this model [18].

In this work we present an analytical generalization of the dipole-dipole interaction model to calculate the maximum vertical repulsive force between a finite permanent magnet and a finite cylindrical superconductor in a perfect Meissner state. We compared our results with experiments and with other calculations. The model applies indistinctly to any compound.

2. The model

In Fig. 1 we show the reference system and geometry used for our calculation. A cylindrical magnet of radius R and thickness L has its uniform volume magnetization $\vec{M} = M\vec{k}$ oriented vertically. The upper base of the magnet lies in the z=0 plane, and a cylindrical superconductor of radius R_s and thickness L_s is coaxially located below the magnet. The gap between magnet and superconductor is a.

We assume that under the magnetic field $\vec{H}(\vec{r})$ produced by the magnet, the superconductor in the Meissner state acquires a volume magnetization $-\vec{H}(\vec{r})/4\pi$, in such a way that $\vec{B}(\vec{r}) = \vec{0}$ in every point inside the superconductor. Here, we shall neglect any demagnetizing effect due to the finite size of the superconducting sample. Such approximation is quite common in the literature, and we believe that this does not affect the relevant features of the system. The perfectly diamagnetic volume dV is equivalent to a dipole of magnetic moment $d\vec{\mu} = -\vec{H}(\vec{r})dV/4\pi$. In this way, the interaction between magnet and superconductor is equivalent to the sum of all the dipole-magnet contributions.

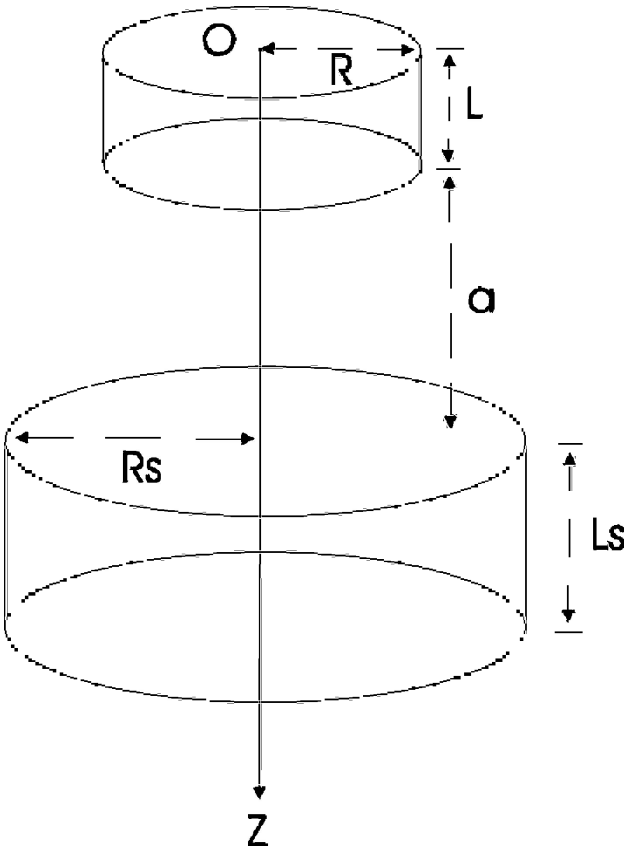

FIGURE 1. Diagram of a cylindrical permanent magnet with uniform magnetization M (parallel to z axis), radius R and thickness L placed a distance a above a cylindrical superconductor of radius Rs and thickness Ls.

Every dipole $d\vec{\mu}$ is subject to an infinitesimal force $d\vec{F}$ due to the magnet, given by:

$$d\vec{F} = \nabla(d\vec{\mu} \cdot \vec{H}) \tag{1}$$

Therefore, by Newton's third law, the total force on the magnet will be $\vec{F} = -\int d\vec{F}$:

$$\vec{F} = \frac{1}{4\pi}\int \nabla[\vec{H}(\vec{r})]^2 dV \tag{2}$$

The integration must be performed over the entire volume of the superconductor.

Now the problem is to evaluate the magnetic field of the magnet. Since there are no electrical currents in the magnet, we can use $\vec{H}(\vec{r}) = -\nabla\Phi(\vec{r})$, where $\Phi(\vec{r})$ is a potential satisfying the Laplace equation. The potential evaluated at points located along the axis of the cylindrical magnet is given by:

$$\Phi(axis) = 2\pi M[\sqrt{(z-L)^2+R^2} - \sqrt{z^2+R^2} + L] \tag{3}$$

Next, we recall a useful property of the solutions to the Laplace equation in the case of azimuthal symmetry [19]. If the function is evaluated in the axis of symmetry and it can be expanded in powers of z (in our case, z is always positive), *i.e.*,

$$\Phi(axis) = \sum_{\ell=0}^{\infty}[A_\ell z^\ell + B_\ell z^{-(\ell+1)}], \tag{4}$$

then the function at any point in space (r,θ) is obtained by substituting z by r and multiplying each power of r^ℓ and $r^{-(\ell+1)}$ by the Legendre polynomial $P_\ell(\cos\theta)$:

$$\Phi(\vec{r}) = \Phi(r,\theta) = \sum_{\ell=0}^{\infty}[A_\ell r^\ell + B_\ell r^{-(\ell+1)}]P_\ell(\cos\theta) \tag{5}$$

Therefore, all we need in order to determine the coefficients A_ℓ and B_ℓ is to expand the potential $\Phi(axis)$ given in Eq. (3) in powers of z.

Once expansion (5) is performed, it is convenient to change from spherical variables (r,θ) to cylindrical variables (ρ,ϕ) before integral (2) is performed. Integration over ϕ gives a factor 2π, and integration over z is reduced to evaluating the integrand at the limits $z_1 = a+L$ and $z_2 = a+L+Ls$. Therefore, we only need to integrate at the variable ρ. All operations were performed using Mathematica.

This method can be followed to calculate the magnetic field produced by magnets with a similar symmetry, rings, spheres, cones, etc.

2.1. Expansion of the potential

There are at least two different regimes of $z > L$ to consider:

(a) $z > L + R$ (far region), where $A_\ell = 0$, $B_\ell \neq 0$, and

(b) $\max(R, L) < z < L + R$ (intermediate region), with $A_\ell \neq 0$, $B_\ell \neq 0$. In addition, if $L < R$, there is a third region:

(c) $L < z < R$ (near region), where $A_\ell \neq 0$, $B_\ell = 0$.

The potential was expanded to a maximum power $\ell = 4$ in the far region. We considered that the convergence of the series with this number of terms was good enough for our purpose. The explicit expression for $\Phi(axis)$ in this region is

$$\Phi(axis) = 2\pi M \left[\frac{LR^2}{2z} + \frac{L^2R^2}{2z^3} + \frac{L^2R^2 - 3LR^3}{16z^4} + \frac{2L^4R^2 - 3L^2R^4}{32z^5} \right]. \quad (6)$$

In this expansion, the constant terms were not included since they disappear in the calculation of the force. When we take the limit corresponding to a small magnet, the leading term of the complete potential in this region is given by

$$\Phi(r, \theta) = \pi M R^2 L \frac{\cos\theta}{r^2}, \quad (7)$$

which corresponds to the potential of a point dipole with magnetic moment $\mu = \pi M R^2 L$ located at the origin. This limit case was discussed extensively in Ref. 11, where the repulsive force F_μ was demonstrated to be

$$F_\mu = \frac{3\mu^2}{8}[g(a) - g(a + L_s)], \quad (8)$$

where

$$g(x) = \frac{1}{x^4} - \frac{R_s^2 + 3x^2}{3(R_s^2 + x^2)^3}. \quad (9)$$

In the intermediate and near regions, the convergence of the series was slower than in the far region. Our criterion was to take as many terms in the series expansion as the computer could handle to calculate the vertical force (up to $\ell = 8$ and $\ell = 7$, respectively). In this way, the series expansion of the potential in the intermediate region is

$$\Phi(axis) = 2\pi M \left[-\frac{R^2}{2z} + z\left(-1 - \frac{L}{R} + \frac{L^3}{2R^3} - \frac{3L^5}{8R^5} + \frac{5L^7}{16R^7}\right) + z^2\left(\frac{1}{2R} - \frac{3L^2}{2R^3} + \frac{15L^4}{16R^5} - \frac{35L^6}{32R^7}\right) + \frac{R^4}{8z^3} + z^3\left(\frac{L}{2R^3} - \frac{5L^3}{4R^5} + \frac{35L^5}{16R^7}\right) + z^4\left(-\frac{1}{8R^3} + \frac{15L^2}{16R^5} - \frac{175L^4}{64R^7}\right) - \frac{R^6}{16z^5} + z^5\left(-\frac{3L}{8R^5} - \frac{35L^3}{16R^7}\right) + z^6\left(\frac{1}{16R^5} - \frac{35L^2}{32R^7}\right) + \frac{5R^8}{128z^7} + z^7\left(\frac{5L}{16R^7}\right) + z^8\left(-\frac{5}{128R^7}\right) - \frac{7R^{10}}{256z^9}\right] \quad (10)$$

Finally, the series expansion of the potential in the near region was

$$\Phi(axis) = 2\pi M \left[z\left(-\frac{L}{R} + \frac{L^3}{2R^3} - \frac{3L^5}{8R^5} + \frac{5L^7}{16R^7}\right) + z^2\left(-\frac{3L^2}{2R^3} + \frac{15L^4}{16R^5} - \frac{35L^6}{32R^7}\right) + z^3\left(\frac{L}{2R^3} - \frac{5L^3}{4R^5} + \frac{35L^5}{16R^7}\right) + z^4\left(\frac{15L^2}{16R^5} - \frac{175L^4}{64R^7}\right) + z^5\left(-\frac{3L}{8R^5} - \frac{35L^3}{16R^7}\right) + z^6\left(-\frac{35L^2}{32R^7}\right) + z^7\left(\frac{5L}{16R^7}\right)\right] \quad (11)$$

As a typical case, we took R=1.25 cm, L=1.5 cm. With these values, we calculated the exact $\Phi(axis)/2\pi M$ from Eq. (3), and compared it with the approximate expansion, Eq. (4). The result is presented in Fig. 2 as a function of the magnet-superconductor separation. As we mentioned above, the potential was expanded to a maximum power $\ell = 4$ in the far region, defined above 1.25 cm. In the intermediate region, defined between 0 and 1.25 cm, the potential was expanded up to $\ell = 8$. The near region was not defined in this case.

The series expansion is discontinuous at R=1.25 cm, *i.e.*, at the boundary between regions. As we shall see, results of the vertical force are poor when part of the superconductor is located on this boundary. For this reason, we shall conclude that our calculation is more reliable when the superconductor lies in a region free of discontinuities, for example in the far region. The final expressions of the force are too long and tedious to write here, therefore we shall use graphics to present its dependence with the geometrical dimensions of the problem.

3. Results and discussion

3.1. Force as a function of the separation

There exist many experimental studies of this type, commonly carried out at 77 K. We shall test the validity of

our model by comparing the calculated force with experimental data [20]. In that work, a melt-textured superconducting sample of YBCO with Rs = 1 cm, Ls= 1 cm, and $Jc(77K)$ around 4×10^5 A/cm^2 was used. The magnet had $M = 829.7G$, R=1.25 cm and L=1.5 cm. Therefore, the potential shown in Fig. 2 corresponds to this magnet. First, we shall discuss the far region ($a > R$).

In Fig. 3, we can see that the maximum possible force calculated with our model is slightly above the experimental result in this region. The highest difference between them is 31%. This means that the sample is able to screen magnetic fields efficiently at large distances. Also, we can say that if

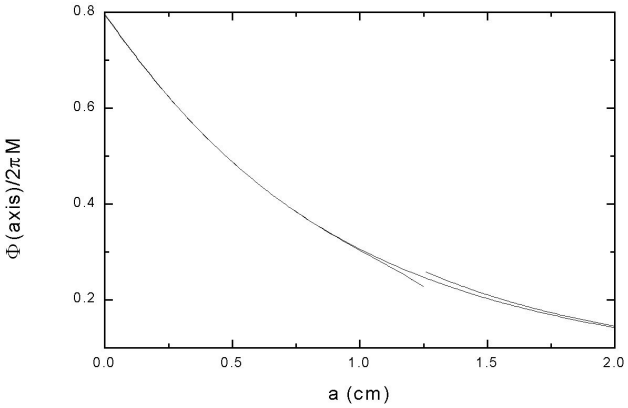

FIGURE 2. Magnetic scalar potential produced by a cylindrical magnet with R=1.25 cm, L=1.5 cm, evaluated along its axis. Continuous line corresponds to the exact expression given by Eq. (3). Dotted line corresponds to the series expansion, Eqs. (6) and (10). The discontinuity of the series at the limit between regions becomes critical when part of the superconductor lies in it, causing a significative error in the calculus.

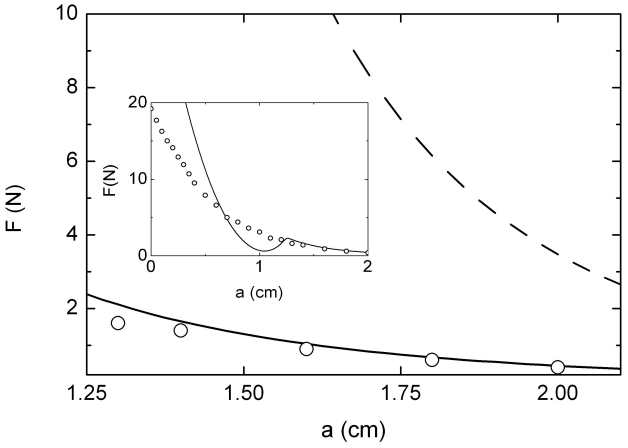

FIGURE 3. Dependence of force on magnet-superconductor separation a in the far region. Circles are experimental data reported in Ref. 13. Continuous line corresponds with our theoretical limit using the potential given in Eq. (6), showing a reasonable agreement with the experiment. The dotted line corresponds to the less realistic result for a magnetic point dipole, Eqs. (8) and (9). The inset shows the force calculated in a wider range of distances including the intermediate region. The bending of the curve is observed around the discontinuity of the potential, see Fig. 2.

the sample is altered to improve the actual force, the increase will be relatively low. This result is particularly important in the design of levitation systems.

As shown in Fig. 3 also, the model of a point dipole located at the same distance, Eqs. (8)-(9), predicts a higher limit. Therefore, our model takes into account the size of the magnet reasonably well, and represents an improved approximation for the maximum force.

The inset of Fig. 3 shows an extended graph over the whole range of distances. The theoretical curve falls between 0.7 and 1.25 cm of separation, as the 1-cm thick superconductor is located partially in the region of discontinuity (around 1.25 cm). The maximum deviation from the original trend is observed at a separation of 1 cm, where the nearest quarter of the sample lies in the problematic area. More terms can be taken in the series expansion to reduce this effect, however the calculation becomes extremely complicated.

As the separation distance is reduced and only the farthest parts of the superconductor remain in the discontinuous zone, the trend of the curve is recovered. But now, magnetic lines start to penetrate the sample and cause it to transit to the mixed state. Because of this, the difference between the experiment and our calculated curve increases. The calculated value at a zero distance is 45 N, a little more than twice the experimental result. Measurements performed at low temperatures would increase the force, and a better agreement is expected.

We tested our model in two more cases. For uniformity, we shall refer to results obtained at a=R. Otani [21] measured F=16.7 N with a SmBCO sample of Jc=7 $\times$ 10^4 A/cm^2, while we predict a 20.3 N value (difference of 21%). Chun *et al.* [5] obtained $F = 0.5N$ for a poor-quality YBCO sample (Jc=3 $\times$ 10^3 A/cm^2), while the maximum expected value is 1.4 N (difference of 180%). We can conclude that our calculation for large distances provides a tool for evaluating the quality of a superconducting sample. Roughly speaking, the calculated repulsive force will reasonably agree with the value measured at 77 K, if Jc is higher than 5 $\times$ 10^4 A/cm^2.

3.2. Dependence of force with the dimensions of the superconductor

Early works [22] showed that the repulsive force increases with the thickness of the superconductor. After a typical initial linear increase, the force lowers the pace until a saturation is reached. We present in Fig. 4 experimental data measured at 77 K by Leblond [20], and our theoretical limit. In this case, parameters are a=0, M=828.7 G, R=1.25 cm, L=1.5 cm, and Rs=1 cm. The superconductor was a YBCO sample with Jc= 20,000 A/cm^2 under a magnetic field of 8 T. The difference between the theoretical values and experimental data is expected, since the sample is penetrated by magnetic lines in the actual experimental conditions. However, we can see that the maximum force predicted with our model has the same trend as the experimental one.

We did not find any experimental work regarding the dependence of the repulsive force on the radius of the superconductor. However, this was modeled in the mixed state by Teshima [3], with Jc as a parameter. In Fig. 5 we present Teshima's results and ours. In this case, the parameters are a=0.1 cm, M=875.4 G, R=1.8 cm, L=2.5 cm, and Ls=2.5 cm. Similarly to the variation with Ls, the repulsive force increases with Rs and saturates to a certain value, which depends on Jc. Our calculated curve with an infinite Jc always remains above the other curves, as it should be.

In summary, the maximum force calculated with our model depends on the dimensions of the superconductor in good correspondence with previous reports. The fact that the force saturates for certain values of Ls and Rs is another important result for designing levitation systems, particularly for optimizing the superconducting material used.

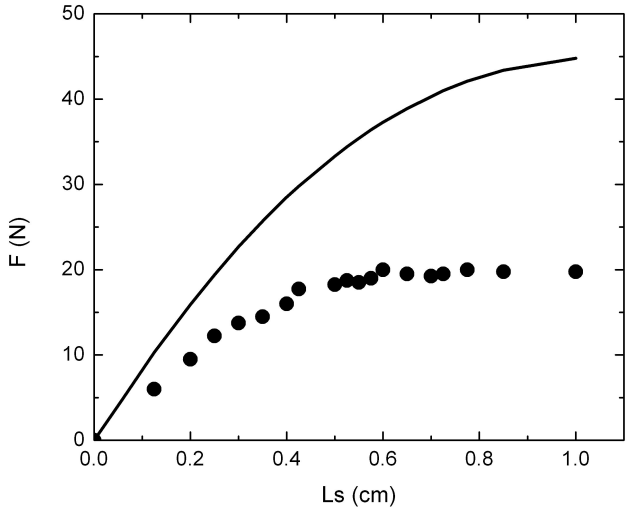

FIGURE 4. Dependence of force on the superconductor thickness Ls. Circles are experimental data reported in Ref. 13 at 77K with a=0. The superconducting sample was made of YBCO and had Jc=2 $\times$ 10^4 A/cm^2 at this temperature under 8 T. Continuous line represents the calculated limit for an infinite Jc.

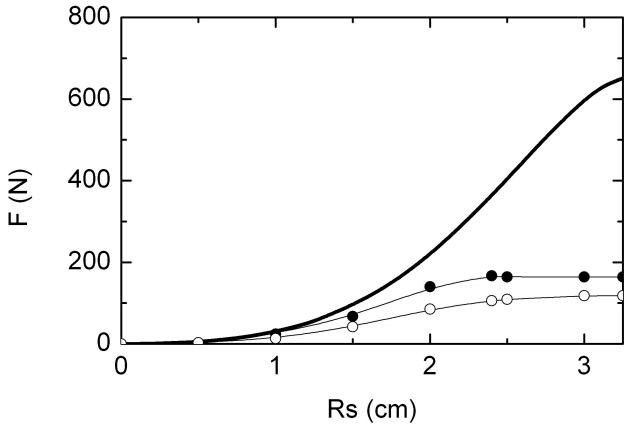

FIGURE 5. Dependence of force on the superconductor radius Rs. Continuous heavy line represents our calculated limit for an infinite Jc. The other curves correspond to calculations published in Ref. 7 in the mixed state at a=0.1 cm. Open circles: Jc=5,000 A/cm^2, filled circles: Jc=20,000 A/cm^2. Continuous light lines are guides for the eye.

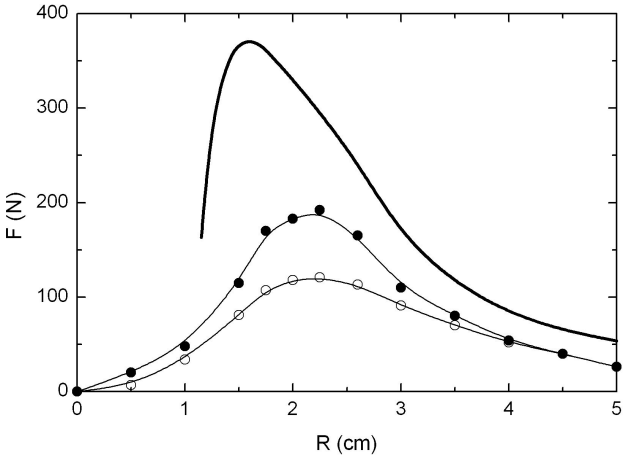

FIGURE 6. Dependence of force on the magnet radius R. Continuous heavy line represents our calculated limit for an infinite Jc. The other curves correspond to calculations published in Ref. 7 in the mixed state at a=0.1 cm. Open circles: Jc=5,000 A/cm^2, filled circles: Jc=20,000 A/cm^2. Continuous light lines are guides for the eye.

3.3. Dependence on the dimensions of the magnet

In this section we analyze the dependence of force on the magnet size. First, we present the influence of the magnet radius in Fig. 6. Teshima's results [3] are included for comparison. The parameters are a=0.1 cm, M=875.4 G, L=2.5 cm, Rs=2.4 cm, and Ls=2.5 cm. It can be seen that, similarly to the dependence on Rs, the force increases and reaches a maximum, depending on the Jc value. However, for larger values of R, the force starts to decrease. The existence of this maximum is a result of the competition between two opposite effects. On one hand, the force trends to grow with the increase of magnetic material. On the other hand, as R becomes larger, the magnetic field produced by the magnet becomes more uniform. Since the force depends on the field gradient, the second effect tends to lower it.

We did not plot the limit curve in Fig. 6 because for small values of R the superconductor lies in a region where the discontinuities of the potential affect the calculation in an important way. This means that our results in this region have a poor confidence.

Finally, we show the dependence of force on the magnet thickness in Fig. 7, using a=0.3 cm, M=780.9 G, R=0.25 cm, Rs=0.5 cm, and Ls=0.48 cm. We calculated this curve in the far region to avoid any discontinuity. It can be seen that F(L) behaves similarly to F(R), *i.e.*, there is a maximum at a certain position. Again, arguments on the opposite effects as a function of L are applied in this case to describe the peak.

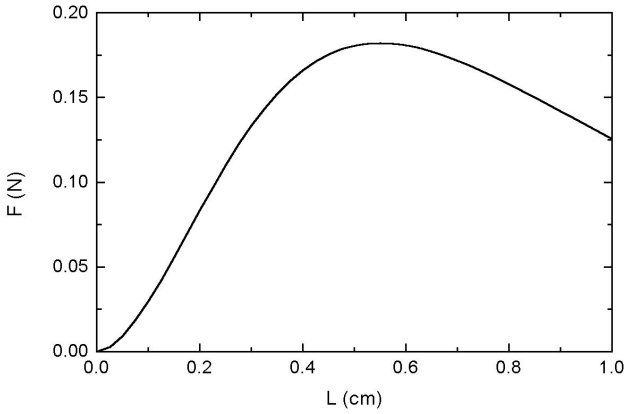

FIGURE 7. Dependence of the force on the magnet thickness L.

4. Conclusions

We developed an analytical method to calculate the maximum possible force between a permanent magnet and a superconductor with azimuthal symmetry in the Meissner state. The magnetic scalar potential was expanded in a power series in three different regions. The application of the method is limited when the superconductor passes through a discontinuity of this series. The basic assumption of the model is that the magnetic field is fully excluded from the superconductor, or equivalently the sample has an infinite critical current density. No experimental parameter other than geometric lengths and magnetization is required. The agreement between theory and experimental data at large distances allows us to use this calculation as a diagnostic tool for the quality of the superconducting sample. In addition, the model describes reasonably well the dependencies of the force on dimensions of the magnet and superconductor. In particular, the force increases monotonically with the size of the superconductor and reaches a saturation value. However, it has a maximum as a function of the magnet dimensions.

Acknowledgements

We wish to thank Lourdes Pinelo for her secretarial assistance. One of us (V. R.-Z.) is grateful for a scholarship from the Academia Mexicana de Ciencias. This work was partially supported by CONACYT-Mexico (Grant No. 34495-E).

∗. Permanent address: CINVESTAV-IPN Unidad Mérida, Apartado Postal 73 CORDEMEX, 97310 Mérida, México. Fax: (999) 981-2917. e-mail: vic@mda.cinvestav.mx

1. F.C. Moon, *Superconducting Levitation*, 1st. ed. (Wiley, New York, 1994).
2. F.C. Moon, *Advances in Superconductivy IV* (Springer-Verlag, 1992) p. 1049.
3. H. Teshima, M. Sawamura, M. Morita, and M. Tsuchimoto, *Cryogenics* **37** (1997) 507.
4. C. Navau and A. Sanchez, *Phys. Rev. B* **58** (1998) 963.
5. Y. Chun and J. Lee, *Physica C* **372** (2002) 1491.
6. F. Hellman, E.M. Gyorgy, D.W. Johnson, Jr., H.M. O'Bryan, and R.C. Sherwood, *J. Appl. Phys.* **63** (1988) 447.
7. Z.J. Yang, Jpn. *J. Appl. Phys. part 2* **31** (1992) L938.
8. Z.J. Yang and J.R. Hull, *J. Appl. Phys.* **79** (1996) 3318.
9. Z.J. Yang, *Solid St. Commun.* **107** (1998) 745.
10. A. Badia and H.C. Freyhardt, *J. Appl. Phys.* **83** (1998) 2681.
11. J. Lugo and V. Sosa, *Physica C* **324** (1999) 9.
12. F.Y. Alzoubi, H.M. Al-khateeb, M.K. Alqadi, and N.Y. Ayoub, *Supercond. Sci. Technol.* **18** (2005) 1329.
13. F.Y. Alzoubi, *Supercond. Sci. Technol.* **19** (2006 248.
14. M.K. Alqadi, F.Y. Alzoubi, H.M. Al-khateeb, and N.Y. Ayoub, *Mod. Phys. Lett. B* **20** (2006) 1549.
15. H.M. Al-Khateeb, M.K. Aldaqi, F.Y. Alzoubi, and N.Y. Ayoub, *Chin. Phys. Lett.* **24** (2007) 2700.
16. F.Y. Alzoubi, M.K. Alqadi, H.M. Al-khateeb, and N.Y. Ayoub, *IEEE Trans. Appl. Supercond.* **17** (2007) 3814.
17. M.K. Alqadi, H.M. Al-khateeb, F.Y. Alzoubi, and N.Y. Ayoub, *Chin. Phys. Lett.* **24** (2007) 2664.
18. F.Y. Alzoubi, H.M. Al-khateeb, M.K. Alqadi, and N.Y. Ayoub, *Chin. Phys. Lett.* **23** (2006) 1641.
19. J.D. Jackson, *Classical Electrodynamics*, 3rd. edition (Wiley, New York, 1975).
20. C. Leblond, I. Monot, D. Bourgault, and G. Desgardin, *Supercond. Sci. Technol.* **12** (1999) 405.
21. T. Otani and M. Murakami, *Supercond. Sci. Technol.* **13** (2000) 866.
22. J. Wang, M. Yanoviak, and R. Raj, *J. Am. Ceram. Soc.* **72** (1989) 846.